Global Atmospheric Carbon Budget: results from an ensemble of atmospheric CO_2 inversions

P. Peylin[1], R. M. Law[2], K. R. Gurney[3], F. Chevallier[1], A. R. Jacobson[4], T. Maki[5], Y. Niwa[5], P. K. Patra[6], W. Peters[7], P. J. Rayner[1,8], C. Rödenbeck[9], I.T. van der Laan-Luijkx[7], X. Zhang[3]

[1]{Laboratoire des Sciences du Climat et de l'Environnement, Gif sur Yvette, France}

[2]{Centre for Australian Weather and Climate Research, CSIRO Marine and Atmospheric Research, Aspendale, Australia}

[3]{School of Life Sciences/Global Institute of Sustainability, Arizona State University, Tempe, USA}

[4]{University of Colorado and NOAA Earth System Research Laboratory, Boulder, USA}

[5]{Meteorological Research Institute, Tsukuba, Japan}

[6]{Research Institute for Global Change, JAMSTEC, Yokohama, Japan}

[7]{Dept. of Meteorology and Air Quality, Wageningen University, Wageningen, Netherlands}

[8]{School of Earth Sciences, University of Melbourne, Parkville, Australia}

[9]{Max-Planck-Institute for Biogeochemistry, Jena, Germany}

Correspondence to: P. Peylin (peylin@lsce.ipsl.fr)

Supplementary material

Description of inversions

A short description of the different inversions is provided below, and a list of stations for each inversion can be found in the section "Observational constraints used by the participating inversion systems", or under: https://transcom.lsce.ipsl.fr.

LSCE_analytical (LSCEa):

LSCEa corresponds to the results described in Piao et al. (2009), the sensitivity test without Siberian vertical profiles. It is based on a "matrix" formulation (see Peylin et al., 2005). ***Fluxes***: solved at the spatial resolution of the transport model and monthly resolution; prior land fluxes taken as the climatology over 1996-2004 from the ORCHIDEE model (Krinner et al., 2005); prior ocean fluxes from Takahashi et al., (2002). Prior land/ocean errors set to 6.0/2.5 Pg C yr^{-1} globally and spatially distributed according to the Gross Primary Production of ORCHIDEE / the surface area of ocean grid cells; flux error correlations between land/ocean grid-points, following an e-folding length of 1000/2000 km. ***Observations***: 73 sites from GLOBALVIEW-CO_2 and CARBOEUROPE EU-project (9 sites); Errors (measurements + model) range between 0.4 ppm for remote stations (South Pole) and 3 ppm for continental sites (Hungaria). ***Prescribed fluxes***: fossil fuel with spatial distribution from Oliver and Berdowski (2001) and annual totals rescaled each year for each country using CDIAC statistics; Biomass burning from van der Werf et al. (2006).

MACC-II version 11.2 from MACC-II project (MACC-II):

MACC-II corresponds to version 11.2 of the CO_2 inversion product from the Monitoring Atmospheric Composition and Climate - Interim Implementation (MACC-II) service (http://www.gmes-atmosphere.eu/). It covers years 1979-2011. An earlier version of this product was described by Chevallier et al., 2010. It is based on a variational formulation with posterior errors provided by a robust Monte Carlo approach. ***Fluxes:*** solved at the spatial resolution of the transport model (Hourdin et al. 2006) and at 8-day daytime/nighttime resolution; the prior fluxes combine estimates of (i) annual anthropogenic emissions (EC-JRC/PBL, EDGAR version 4.2, http://edgar.jrc.ec.europa.eu/, 2011, http://cdiac.ornl.gov/ftp/ndp030/global.1751 2008.ems, accessed 6 July 2011, and http://cdiac.ornl.gov/trends/emis/meth reg.html, accessed 8 January 2013), climatological monthly ocean fluxes (Takahashi et al., 2009), climatological monthly biomass burning emissions (taken as the 1997–2010 mean of the database of van der Werf et al., 2010) and climatological 3-hourly biosphere-atmosphere fluxes taken as the 1989–2010 mean of a simulation of the ORCHIDEE model (Krinner et al., 2005), version 1.9.5.2. These gridded prior fluxes exhibit 3-hourly variations but their inter-annual variations are caused by anthropogenic emissions only. Prior land/ocean errors are set to 2.8/0.75 PgC y^{-1} globally and spatially distributed according to the heterotrophic respiration of ORCHIDEE / the surface area of ocean grid cells; flux error correlations between land/ocean grid-points, following an e-folding length of 500/1000 km. ***Observations:*** 134 sites from a series of global databases; Errors (measurements + model) range between a few tenths of a ppm for marine stations and up to 6 ppm for continental sites (CBW).

CarbonTracker US (CT2011_oi):

CarbonTracker is an ongoing program of the United States National Oceanic and Atmospheric Administration (NOAA) to publish approximately-annual estimates of CO_2 surface exchange over the globe. The 2011 update of CarbonTracker (CT2011_oi) used here is a revised version of the system described in Peters et al. (2007) and is fully documented online at http://www.esrl.noaa.gov/gmd/ccgg/carbontracker/CT2011_oi/.

CarbonTracker uses an ensemble Kalman filter scheme to estimate weekly scaling factors multiplying prior-model net carbon exchange over 126 land and 30 ocean regions covering the globe. Flask and quasi-continuous observations from 94 sites of the CO_2 observing networks operated by NOAA, Environment Canada, the Australian Commonwealth Scientific and Industrial Research Organization (CSIRO), the National Center for Atmospheric Research (NCAR), the Brazilian Instituto de Pesquisas Energéticas e Nucleares (IPEN), and Lawrence Berkeley National Laboratory are assimilated to produce optimal surface flux estimates. A relatively short assimilation window of five weeks is used to determine adjustments to surface fluxes. Model-data mismatch errors assigned to observations range from 0.75 to 7.5 ppm. Atmospheric transport is simulated with the nested-grid TM5 model described in Krol *et al.* (2005), using winds from the operational forecast model of the European Centre for Medium-Range Weather Forecasts.

CarbonTracker simulates four types of CO_2 exchange with the atmosphere. Fossil-fuel and biomass burning estimates are imposed without modification, and air-sea exchange and non-wildfire land exchange are subject to optimization.

In an attempt to estimate uncertainties stemming from the use of biased flux prior models, CT2011_oi uses two fossil fuel emissions estimates ("Miller" and ODIAC) and two land biosphere (GFEDv2 and GFEDv3) emissions estimates (natural exchange plus biomass burning). A 2x2 factorial expansion yields four independent inversions, each using a unique combination of these priors. The 1ˇx1ˇ monthly fluxes used in this manuscript are the across-model mean of these four inversion flux estimates:

- **Fossil Fuel emissions:** i) based on annual totals for each country from Carbon Dioxide Information and Analysis Center (CDIAC) estimates from 2000 to 2008 and the BP Statistical Review of World Energy; and ii) based on Open-source Data Inventory for Anthropogenic CO_2 (ODIAC, Oda and Maksyutov, 2011), updated for use in CarbonTracker.
- **Land biosphere priors** are supplied by two versions of the Carnegie-Ames-Stanford Approach (CASA) biogeochemical model used to create the Global Fire Emissions Database (GFED; van der Werf *et al.*, 2006).

Details of the flux modules are available at http://carbontracker.noaa.gov. Compared to the CT2007 release described in Peters *et al.* (2007), the following significant changes have been made in CT2011_oi: i) observations from 29 new datasets have been used as assimilation constraints; ii) seasonality of fossil fuel emissions has been extended to the entire Northern Hemisphere north of 30ˇN; iii) the air-sea CO_2 flux prior is now time-varying and comes from the ocean inversions reported in Jacobson *et al.* (2007), and iv) a suite of four independent inversions using different combinations of prior flux models is now used to produce the CarbonTracker estimates. The number of ocean regions has been increased to 30 from its original 11. The resolution of atmospheric transport in the global domain has been increased to 3ˇx2ˇ (N. American transport remains at 1ˇx1ˇ).

CarbonTracker Europe (CTE2013):

CarbonTracker Europe is based on a similar inversion framework as CarbonTracker US described above. It differs in a number of important choices for the inputs, specifically:

- CTE2013 uses a more extensive set of European CO_2 mole fraction observations not assimilated in CT2011_oi. These are derived from obspack_co2_1_-PROTOTYPE_v1.0.3_2013-01-29,
- Fire fluxes and the associated monthly mean biosphere fluxes come from a climatological extension of GFED2 (2000-2007) to the years 2008, 2009, and 2010,
- CTE2013 uses a TM5 two-way nested transport on a 3x2 degrees grid with highest 1x1 degree resolution over Europe as well as over North America. The European zoom domain uses interpolated meteorological fields from the 3x2 degrees parent grid,
- CTE2013 uses only one inversion flux estimate and not a mean of several estimates based on different priors.

Details of CTE2013 are available at http://www.carbontracker.eu/.

CCAM and MATCH:

The CCAM and MATCH inversions use a Bayesian synthesis method and are described in Rayner et al. (2008), except that the time period of the inversions has been extended to 2008 and a slightly different set of observing sites has been used. The CCAM and MATCH inversions set up is identical except for the transport model used (CCAM or MATCH) and the number of regions solved for (CCAM: 94 land, 52 ocean, MATCH: 67 land, 49 ocean). Neither transport model used interannual-varying winds. ***Fluxes:*** Land fluxes are solved relative to a CASA climatology (Randerson et al., 1997). Most land priors are zero relative to CASA with some non-zero priors representing land-use change. Ocean fluxes are solved relative to the climatology of Takahashi et al. (1999) with prior fluxes of zero. Prior land uncertainties are scaled by NPP while ocean uncertainties are scaled by region area with total uncertainty similar to Baker et al. (2006). ***Prescribed fluxes*:** fossil emissions follow a spatial distribution which is a linear combination of Andres et al. (1996) representing 1990 and Brenkert (1998) representing 1995, scaled to annual totals from CDIAC. ***Observations:*** 73 CO_2 records from GLOBALVIEW-CO2 (2009), used as monthly means, 7 $\delta^{13}CO_2$ records from CSIRO (Francey et al., 1996).

Data uncertainties range from 0.3-9.2 ppm and vary in time. Larger uncertainties are used for periods with extrapolated data from GLOBALVIEW.

JENA s96-v3.5 (JENA):

The Jena inversion has been designed with the focus to estimate interannual variations of land and ocean CO_2 fluxes. Data records are selected to span the whole inversion period (1996-2011), to avoid spurious variations from network changes. In order to make the estimated interannual variations directly traceable to the atmospheric signals, interannual variations in land/ocean prior fluxes are avoided. ***Observations***: CO_2 mixing ratio data from 50 sites. Flask pair values or hourly values, respectively, are used directly at their time of measurement. Hourly data are selected for day-time or night-time values at certain sites (see Table at the end of the Supplementary material). ***Fluxes***: Estimated at the spatial resolution of the transport model and daily time steps, but with a-priori spatial and temporal correlations (decaying with distance). Land fluxes are adjusted in the mean and at roughly weekly to interannual time scales, with extra degrees of freedom for large-scale seasonality. Land flux adjustments are spatially weighted with a productivity proxy (long-term mean NPP from the LPJ model). Ocean fluxes are only adjusted at weekly to interannual time scales, while the mean spatial pattern is taken from the prior based on oceanic data. ***Prior fluxes***: Fossil fuel emissions: EDGAR 4.0 (linearly extrapolated after 2005 using BP global totals). Land: Time-mean spatial pattern of NEE from LPJ model. Ocean: Sum of the ocean uptake flux induced by the anthropogenic perturbation as compiled by Mikaloff-Fletcher et al. (2006), the preindustrial air-sea fluxes from Mikaloff-Fletcher et al. (2007), and the river fluxes of Jacobson et al. (2007); seasonality from Takahashi et al. (2002). ***Solution method:*** Conjugate Gradients minimization with re-orthonormalization after each iteration.

Jena inversion runs are also available for longer time periods (starting 1981 using 14 long-record sites), or using more sites (up to 79, for shorter periods over which all sites provide data). All results, including regular updates, can be downloaded from “http://www.bgc-jena.mpg.de/~christian.roedenbeck/download-CO2/”.

TRANSCOM_mean (TrC):

The TransCom mean results are based on the TransCom 3 Level 2 analysis found in Gurney et al. (2008) and Baker et al., 2006, but the observational time series have been extended to 2008 (inclusive). The individual posterior flux results (from 11 transport models) are averaged to generate the multi-model mean. The observational time series spans the 1990 to 2008 time period with a total of 103 observing sites from the GLOBALVIEW-CO_2 database. The inversion approach used in the TransCom 3 Level 2 results follows the Bayesian synthesis method (Enting 2002). There are 11 land and 11 ocean basis functions that are roughly sub-continental in size. The four background carbon fluxes consisted of 1990 and 1995 fossil fuel emission fields (Andres et al., 1996; Brenkert, 1998), an annually-balanced, seasonal biosphere exchange (Randerson et al., 1997), and air-sea gas exchange (Takahashi et al., 1999). These fluxes are included in the inversion with a small prior uncertainty so that their magnitude is effectively fixed.

RIGC TDI-64 (RIGC):

This Bayesian time-dependent inversion with 64-regions (**TDI-64**) is developed based on the TransCom level 3 inverse model in order to increase the degrees of freedom for flux estimation (or reduce regional aggregation error). The 11 land and 11 ocean regions are divided into 42 and 22 regions, respectively (detailed sensitivity tests for prior flux and data uncertainties/network are discussed in Patra et al. (2005). By this division, we are able to draw distinction between the east and west or north and south of 10 TransCom land regions, and north and south of the Tropical Asia and all ocean regions. **Atmospheric CO_2** time series from 74 GLOBALVIEW-CO2 sites are used with their corresponding uncertainty derived from climatology of the monthly mean residuals plus 0.3 ppm as a measure of the model representation error. The data uncertainty varies from 0.31 ppm at South Pole (SPO) to 4.6 ppm at the Hungarian tower (HUN) and 5.1 ppm at BSC. The NIES/FRCGC **transport model** (Maksyutov et al., 2008) is driven by interannually-varying NCEP reanalysis meteorology. The **pre-subtracted fluxes** are taken from CASA terrestrial ecosystem model (Randerson et al., 1997) (i.e., monthly biosphere fluxes with no net annual sink are imposed to the inversion system like fossil fuel emissions to account for the seasonal carbon fluxes from the vegetation) and Takahashi et al. (2009) climatology for oceanic exchange at monthly time intervals. Fossil fuel emission distributions are taken from EDGAR4.0 and global totals are scaled to CDIAC estimated annual emissions. Prior flux uncertainties are assigned in range of ~0.37 $PgCy^{-1}$ to ~2.12 $PgCy^{-1}$ for both land and ocean regions.

JMA 2010 (JMA):

JMA inversion method corresponds to the method described in Maki et al. 2010 which is based upon TransCom 3 IAV inversion set up (Baker et al. 2006) with raw observation data (WDCGG) and interannually-varying wind (JRA25 and JCDAS). The analysis period is extended to 2009 and a vertical mixing problem in our transport model (JMA-CDTM) is fixed. ***Fluxes:*** solved at the spatial resolution of 22 regions and on monthly basis; prior land fluxes taken as the climatology from CASA model; prior ocean fluxes from Takahashi et al., (2002). Prior land/ocean errors set to TransCom 3 IAV uncertainties; flux error correlations are set to zero. ***Observations:*** 146 sites from WDCGG monthly mean CO_2 concentrations after site selection by mismatch between observation and inversion; Errors (measurements + model) range between 0.3 ppm for remote stations (SPO) and 5 ppm for continental sites. ***Prescribed fluxes:*** fossil fuel emissions with spatial distribution from Andres et al. (1996) and Brenkert (1998) annual totals rescaled each year for each country using CDIAC statistics.

NICAM-TM (NICAM):

NICAM-TM inversion system is described by Niwa et al. (2012). While Niwa et al. (2012) extensively used aircraft measurements from CONTRAIL (observations from Airliners, http://www.cger.nies.go.jp/contrail/contrail.html) the NICAM inversion shown in this study used only surface measurements and few aircraft measurements. The inversion method and setup are similar to those of TransCom. ***Fluxes***: the spatial number of fluxes solved by the inversion is 29 and 11 respectively for land and ocean. The 29 land regions were obtained by dividing the 11 regions of TransCom (slightly different from 31 regions of Niwa et al. (2012)). The ocean flux region definition is the same as TransCom. The prior land flux is taken from the climatology flux of CASA (Randerson et al. 1997); the prior ocean flux is from Takahashi et al., (2009). Prior land flux errors are given by redistributing those for the 11 regions of TransCom into the 29 regions according to NPP distributions, whereas prior ocean flux errors are the same as those of TransCom. There is no error correlation for the prior fluxes**.** ***Observations***: 71 sites from

GLOBALVIEW-CO_2, which consist of the same 59 surface sites as those used by Niwa et al. (2012) and 12 aircraft measurement points of CONTRAIL between Japan and Australia; Errors (measurements + model) range between 0.3 ppm for remote stations and 6.6 ppm for continental sites (LEF) (monthly mean). ***Prescribed fluxes***: fossil fuel with spatial distribution from EDGAR version 4.1 and annual totals rescaled each year for each country using CDIAC statistics.

Additional figures

This appendix provides additional figures showing the estimated and prior aggregated carbon fluxes (Figures S1 to S6) as well as the region boundaries used to aggregate the fluxes (Figure S7) and the spatial flux distribution (Figure S8).

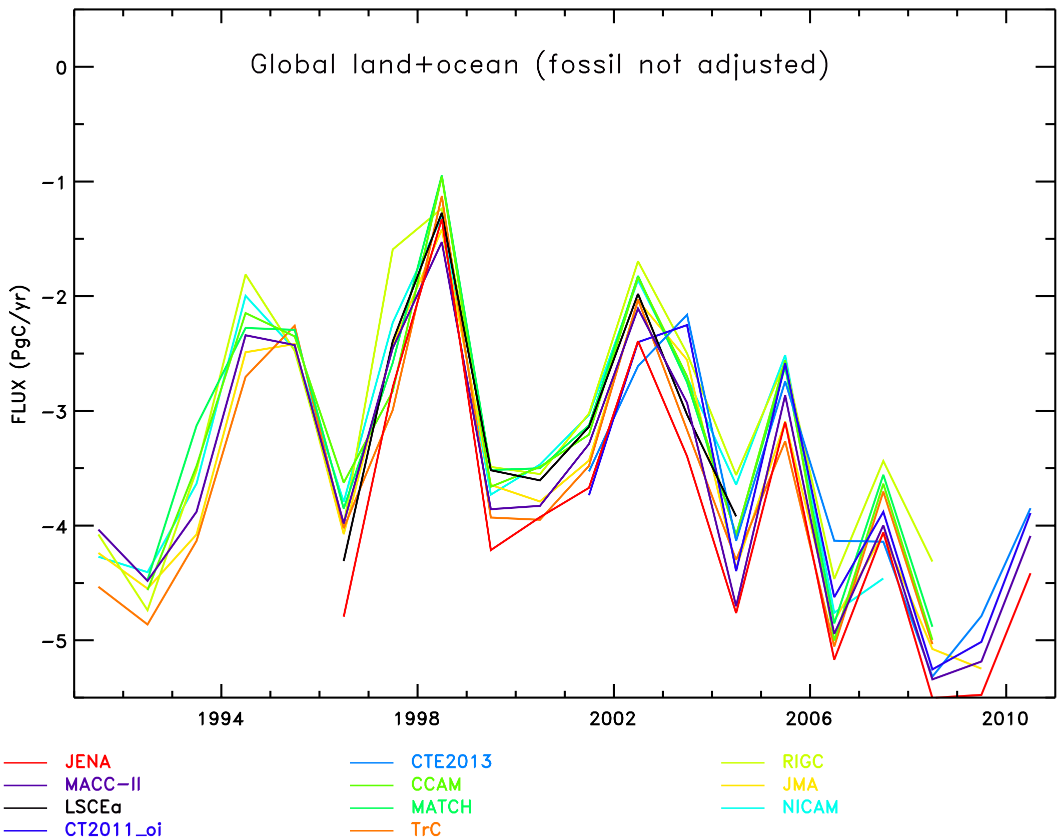

Figure S1: Annual mean posterior flux of the individual participating inversions for natural global total carbon exchange without fossil correction.

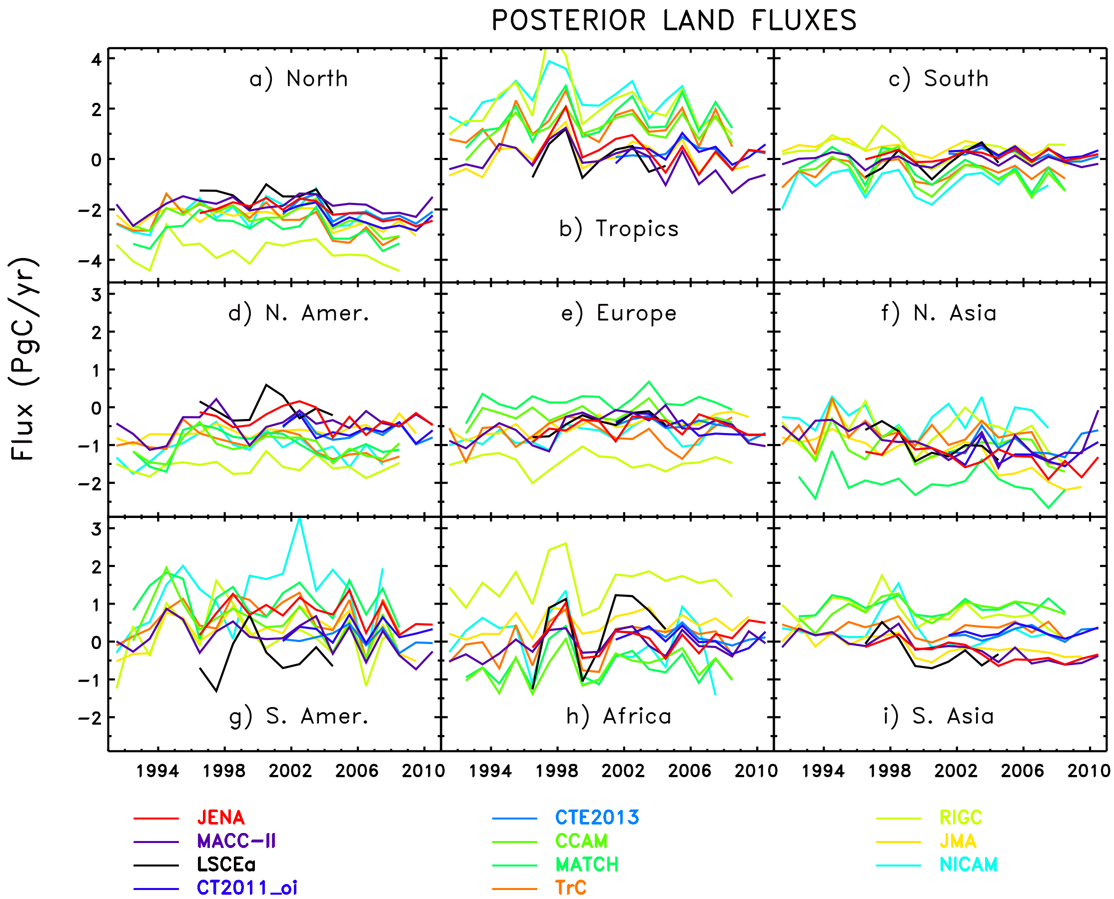

Figure S2: Annual mean posterior natural land flux estimate of the individual participating inversions. Shown here are a) North (>25N) b) Tropics (25S<<25N), c) South (<25S) d) North America, e) Europe, f) North Asia, g) South America, h) Africa, i) South Asia.

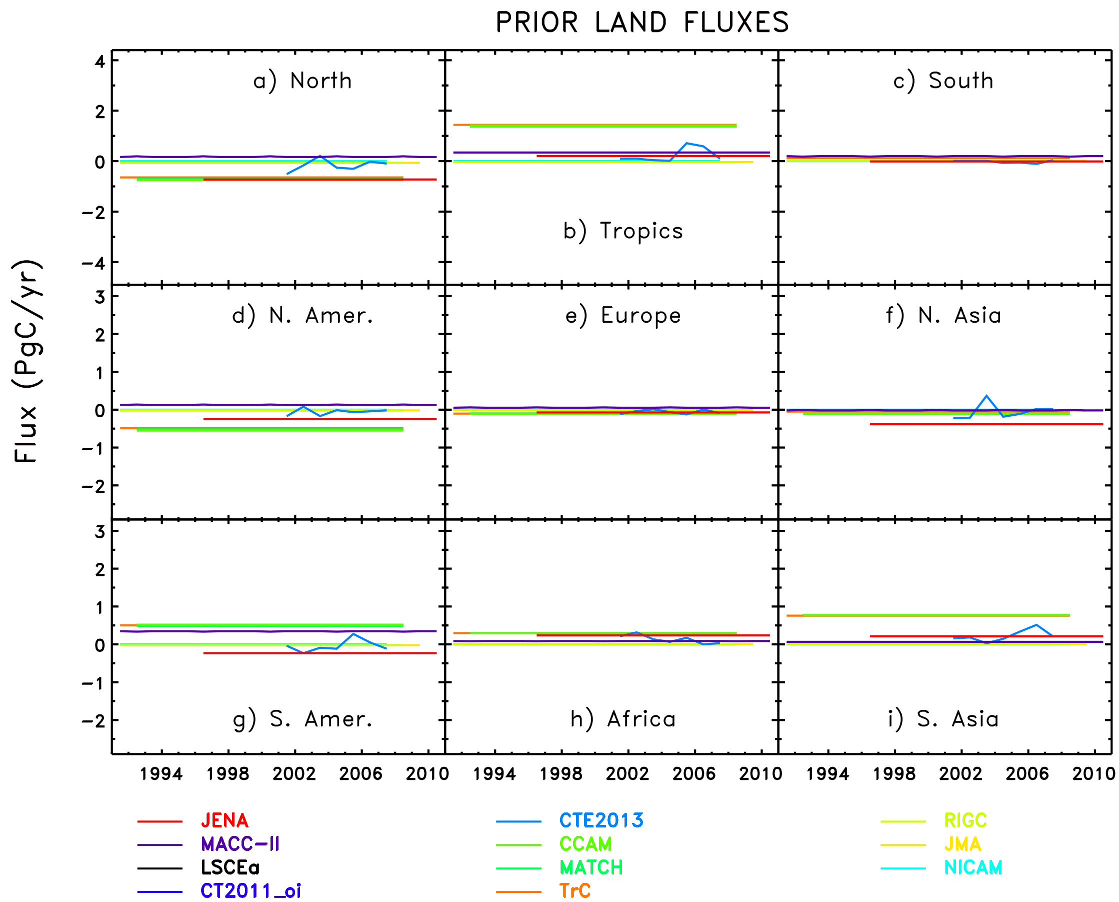

Figure S3: Same as Fig. S2 but for the Prior land fluxes.

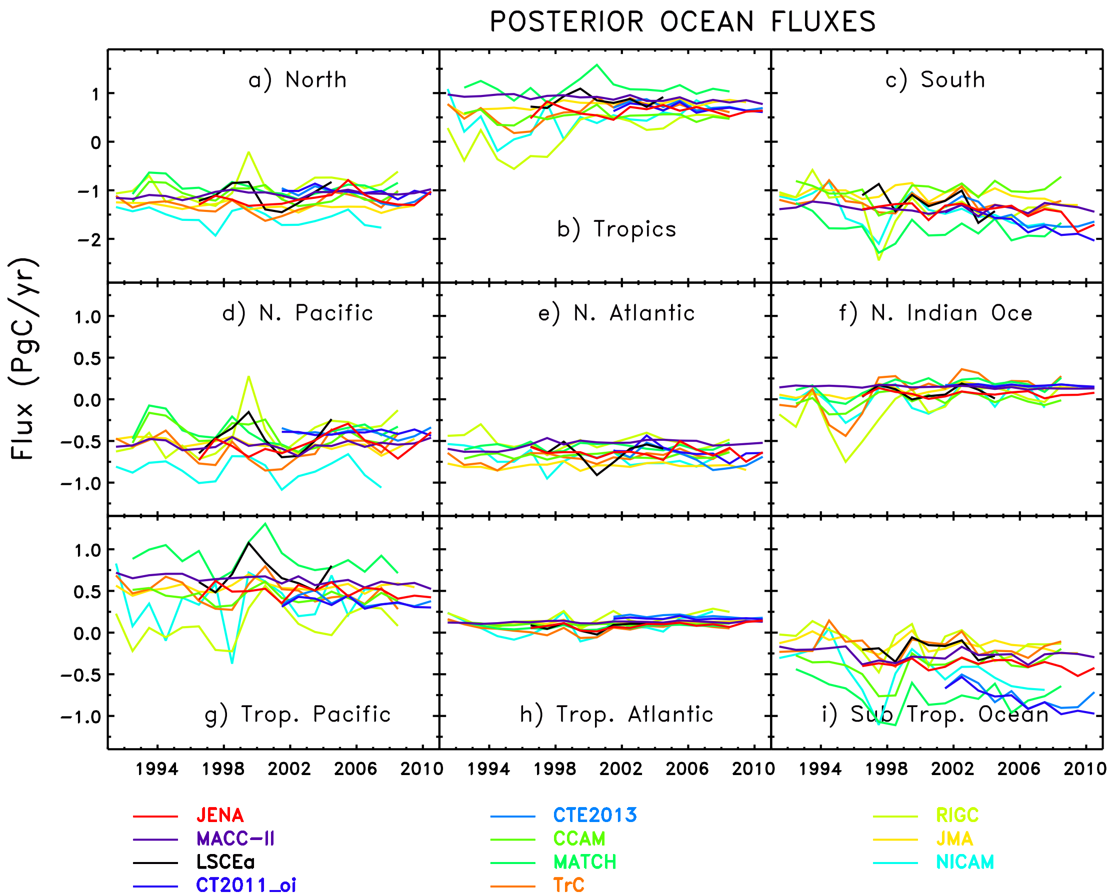

Figure S4: Annual mean posterior natural ocean flux estimate of the individual participating inversion. Shown here are a) North (>25N) b) Tropics (25S<<25N), c) South (<25S) d) North Pacific, e) North Atlantic, f) Tropical Indian ocean, g) Tropical Pacific, h) Tropical Atlantic, i) Sub tropical ocean.

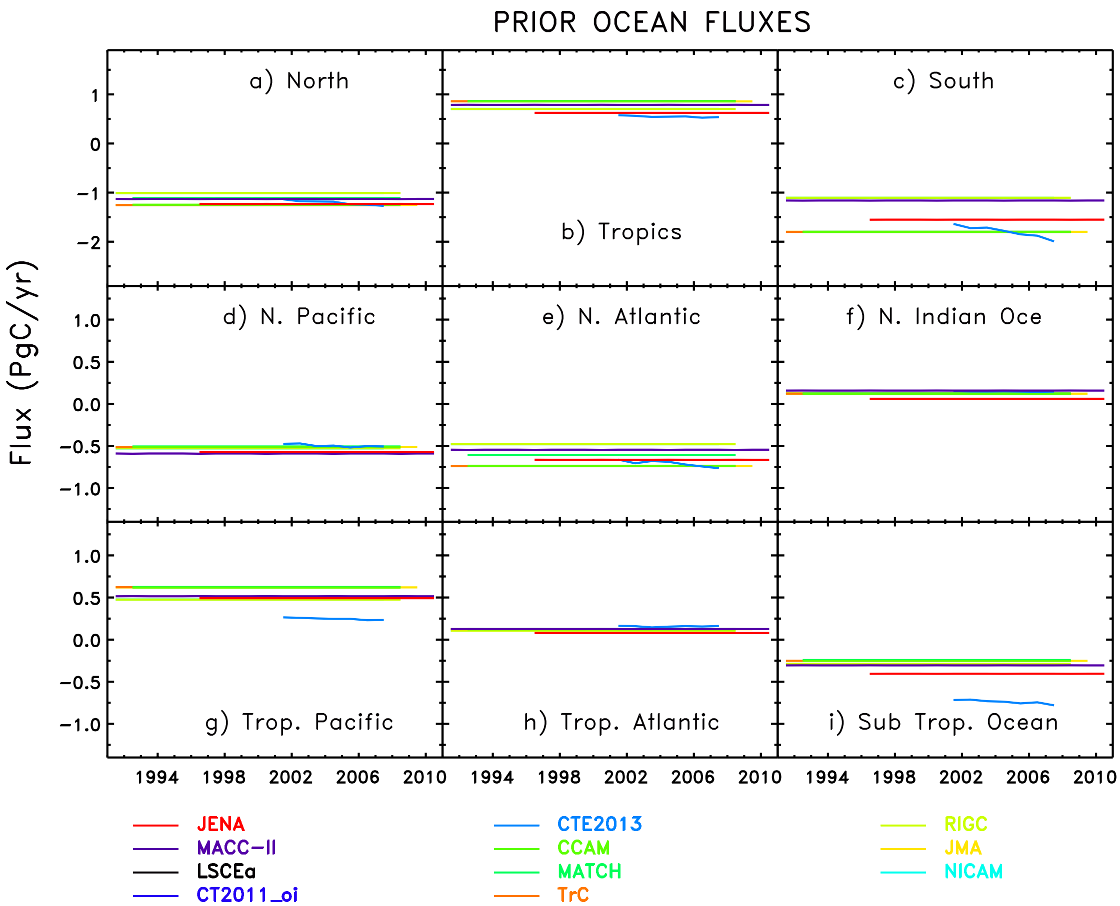

Figure S5: Same as Fig. S4 but for the Prior ocean fluxes.

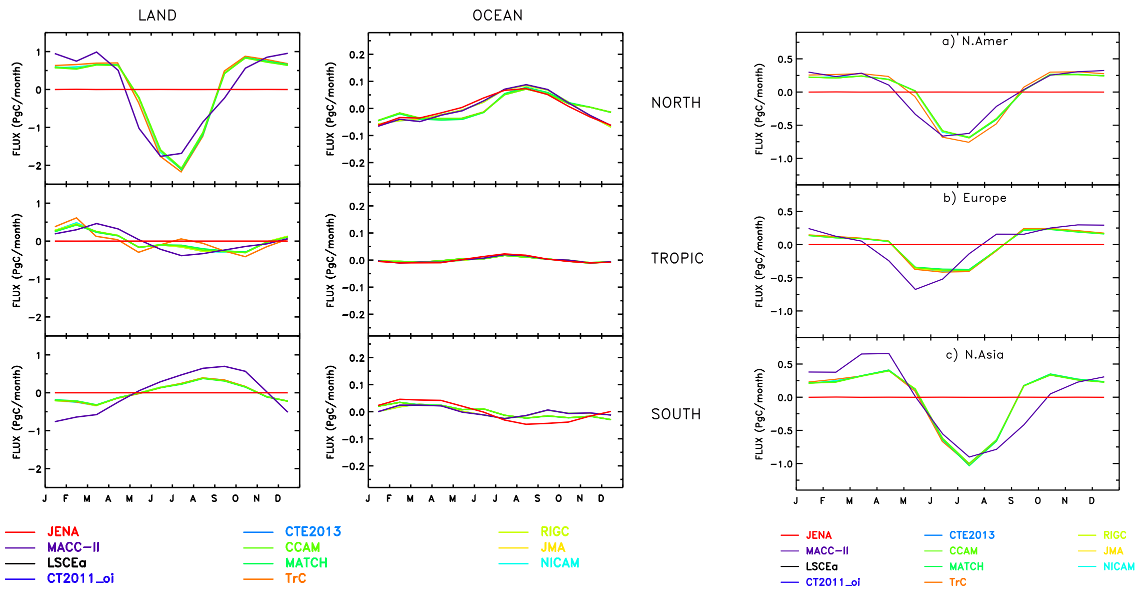

Figure S6: Mean seasonal cycle for the prior fluxes from most participating models for selected regions

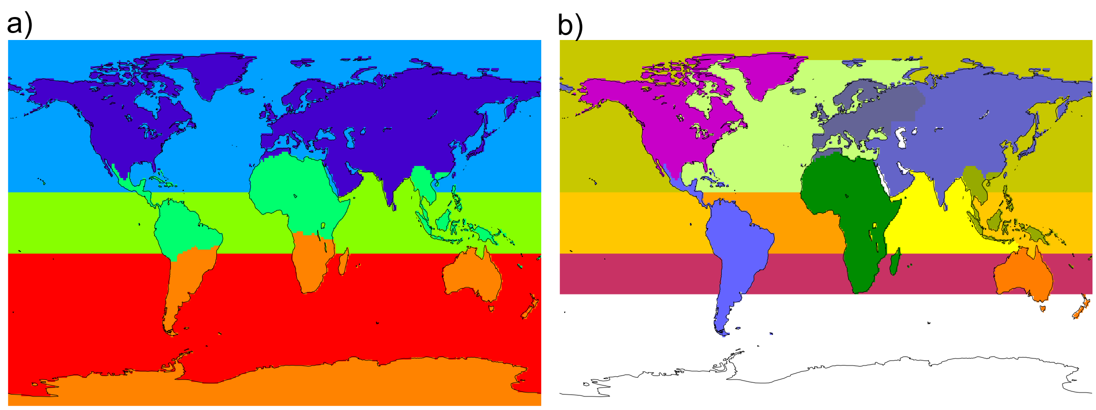

Figure S7: Region boundaries used for the aggregated fluxes: a) latitudinal breakdown (north, tropics, south) for land and ocean; b) continental breakdown used for north America, Europe, north Asia, south America, Africa, tropical Asia, Australia, north Pacific, north Atlantic, tropical pacific, tropical Atlantic, Indian ocean, sub-tropical ocean.

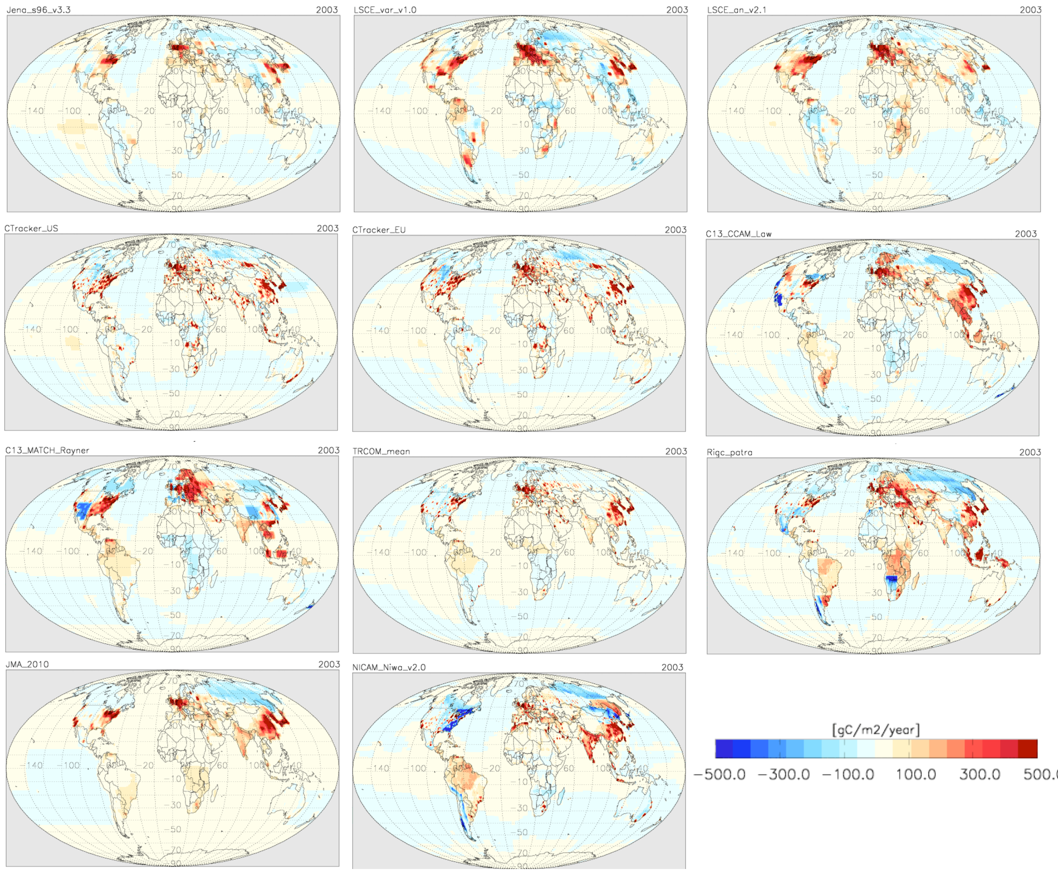

Figure S8: Spatial distribution of the annual natural fluxes (without fossil correction) for 2003 for the participating inversions.

Observational constraints used by the participating inversion systems

Sites are listed alphabetically, in general using the site codes of GLOBALVIEW (www.esrl.noaa.gov/gmd/ccgg/globalview/co2/co2_observations.html). Many site locations are listed more than once, since multiple CO_2 records are available for many sites (either collected by different labs, or representing separate flask and in-situ records). Some inversions chose only to use the most complete record at a given location while others include all available records. It is unlikely that one choice is better than the other. There are differences in calibration etc between laboratories. These are not accounted for in inversions, but their impact is unlikely to be significant compared to other transport and representation uncertainties in modelling any given site (Rödenbeck et al., 2006).

Type of observed CO_2 used for each site: There are a variety of ways the CO_2 data from any given site has been used, depending in part on whether flask or in-situ data are available; some inversions use monthly mean data while others use the data at the appropriate sampling time. Various degrees of selection have been applied to the data. An indication of how the data have been used is given in the table through a series of codes.

Table 1: Codes describing the way observations are used.

Code	Explanation
Temporal resolution	
M	Monthly mean data used
D	Daily mean data used
H4	Four hour mean data used
H4 (hrs)	Four hour mean data used only for the hours indicated (UT)
H	Hourly data used
H (hrs)	Hourly data used only for the hours indicated (UT)
F4	Flask samples are used as a 4 hour average around sampling time
F	Flasks samples are used at the sampling time
Data selection	
GV	Globalview CO_2 used. Globalview CO_2 is derived from a fitted curve to CO_2 observations and is intended to represent baseline conditions; used as monthly mean data
GV E	The use of Globalview CO_2 data includes extrapolated data. This fills in missing data by applying a mean seasonal offset for the site from marine boundary layer CO_2 concentration. Many inversions give periods of extrapolated data less weight than periods with observations.
*	Consecutive hours that differ by greater than 1 ppm are removed
o	Outliers (mismatch between observations and model > 3 sigma) are removed
JMA	Data are removed when inconsistent with the inversion through an iterative procedure (Maki et al., 2010)

Site locations may be represented by model output interpolated to the site location or by the nearest model grid-cell. For coastal sites, the nearest ocean grid-cell if often chosen as being more representative of the baseline air that is usually sampled by flask records at coastal sites.

Some inversions include ship data. This may be used at the actual location and time of sampling (as in the CarbonTracker inversions) or it may be binned into latitude and/or longitude bins as in the GLOBALVIEW POC* records and the JMA use of JMA ship data.

Table S2: List and description of the sites used by each inversion system.

Site name[a]	Laboratory[b]	Lon	Lat	TRCom	CCAM	MATCH	RIGC	JENA s96_v3.5	MACC-II	NICAM -TM	CT2011 _oi	CTE2013	JMA	LSCE ana
ABP	NOAA F	-38.17	12.77								F4o	F4o		
ABP	IPEN F	-38.17	12.77								F4o			
ALT	NOAA F	-62.52	82.45	M GV E	M GV E	M GV E	M GV E	F	F		F4o		M JMA	M GV
ALT	CSIRO F C13	-62.52	82.45		M	M								
ALT	CSIRO F	-62.52	82.45	M GV E				F						
ALT	EC F	-62.52	82.45	M GV E				F						
ALT	EC I	-62.52	82.45	M GV E					H(12-20)	M GV E	H4(12-16)o	H4(12-16)o		
ALT	SIO F	-62.52	82.45	M GV E										
AMS	LSCE I	77.53	-37.95		M GV E	M GV E	M GV E		H(12-20)					M GV
AMS	LSCE F	77.53	-37.95						F					
AMS	NOAA F	77.53	-37.95						F				M JMA	
AMT107	NOAA I	-68.68	45.03						H(12-20)		H4(12-16)o	H4(12-16)o		
AMT_01P0 (107m)	NOAA F	-68.68	45.03								F4o			
AMY	KMA I	126.32	36.53						H(12-20)					
ASC	NOAA F	-14.42	-7.92	M GV E	M GV E	M GV E	M GV E	F	F	M GV E	F4	F4	M JMA	M GV
ASK	NOAA F	5.42	23.18	M GV E	M GV E	M GV E	M GV E	F	F	M GV E	F4o	F4o	M JMA	M GV
AVI	NOAA F	-64.75	17.75						F				M JMA	
AZR	NOAA F	-27.38	38.77	M GV E	M GV E	M GV E	M GV E	F	F	M GV E	F4o	F4o	M JMA	M GV
BAL	NOAA F	16.67	55.50	M GV E	M GV E	M GV E	M GV E	F	F	M GV E	F4o	F4o		
BAO300	NOAA I	-105.00	40.05								H4(12-16)o	H4(12-16)o		
BAO_01PO (300m)	NOAA F	-105.00	40.05								F4o			
BER	MGO F	165.98	55.20						FD					
BGU	LSCE F	3.33	41.83						F			F4o		

Site name[a]	Laboratory[b]	Lon	Lat	TRCom	CCAM	MATCH	RIGC	JENA s96_v3.5	MACC-II	NICAM -TM	CT2011 _oi	CTE2013	JMA	LSCE ana
BHD	NIWA I	174.87	-41.41	M GV E	M GV E	M GV E			F	M GV E				
BHD	SIO F	174.87	-41.41					F						
BHD	NOAA F	174.87	-41.41						F		F4o	F4		
BIK0300	MPI- BGC	22.75	52.25											
BKT	NOAA F	100.32	-0.20						F		F4o	F4o		
BME	NOAA F	-64.65	32.37	M GV E	M GV E	M GV E	M GV E		F		F4o	F4o	M JMA	
BMW	NOAA F	-64.88	32.27	M GV E			M GV E	F	F	M GV E	F4o	F4o		M GV
BRA	EC I	-104.7	51.2									H4(12-16)o		
BRW	NOAA I	-156.60	71.32	M GV E	M GV E	M GV E	M GV E	H*	H(12-20)	M GV E	H4(12-16)o	H4(12-16)o	M JMA	M GV
BRW	NOAA F	-156.60	71.32	M GV E				F	F		F4o			
BRW	SIO F	-156.60	71.32					F						
BSC	NOAA F	28.68	44.17	M GV E	M GV E	M GV E	M GV E				F4o	F4o		
BZH	LSCE F	-4.67	48.58						F					
CAR03000	NOAA F	-104.80	40.90	M GV E			M GV E							
CAR04000	NOAA F	-104.80	40.90	M GV E	M GV E	M GV E	M GV E							MGV
CAR05000	NOAA F	-104.80	40.90	M GV E										
CAR06000	NOAA F	-104.80	40.90	M GV E	M GV E	M GV E	M GV E							
CAR07000	NOAA F	-104.80	40.90	M GV E										
CAR08000	NOAA F	-104.80	40.90	M GV E										M GV
CBA	NOAA F	-162.72	55.20		M GV E	M GV E		F	F		F4o	F4o	M JMA	M GV
CBA	SIO F	-162.72	55.20	M GV E			M GV E	F		M GV E				
CBW0200	ECN I	4.90	52.00						H(12-20)					
CDL030	EC I	-104.65	53.87						H(12-20)		H4(12-16)o	H4(12-16)o		
CFA	CSIRO F	147.06	-19.28	M GV E	M GV E	M GV E	M GV E	F	F	M GV E	F4o	F4o	M JMA	M GV
CFA	CSIRO F C13	147.06	-19.28		M	M								
CGO	NOAA F	144.68	-40.68	M GV E	M GV E	M GV E	M GV E	F	F	M GV E	F4	F4		M GV
CGO	CSIRO F	144.68	-40.68	M GV E				F			F4		M JMA	

Site name[a]	Laboratory[b]	Lon	Lat	TRCom	CCAM	MATCH	RIGC	JENA s96_v3.5	MACC-II	NICAM -TM	CT2011 _oi	CTE2013	JMA	LSCE ana
CGO	CSIRO F C13	144.68	-40.68		M	M								
CGO	SIO F	144.68	-40.68	M GV E										
CHM	EC I	-74.3	49.68									H4(12-16)o		
CHR	NOAA F	-157.17	1.70		M GV E	M GV E		F	F	M GV E	F4	F4	M JMA	M GV
CHR	SIO F	-157.17	1.70					F						
CIB	NOAA F	-4.93	41.81									F4o		
CMN	IMS I	10.70	44.18	M GV E	M GV E	M GV E	M GV E	H*(23-5)	H(1-6)	M GV E				M GV
CMO	NOAA F	-123.97	45.48						F				M JMA	
COI	NIES I	145.50	43.15	M GV E	M GV E	M GV E			H(12-20)					
CPT	SAWS I	18.49	-34.35	M GV E	M GV E	M GV E	M GV E	H*(11-17)	H(12-20)	M GV E		D0	M JMA	M GV
CRZ	NOAA F	51.85	-46.45	M GV E	M GV E	M GV E	M GV E		F	M GV E	F4	F4	M JMA	M GV
CSJ	EC F	-131.02	51.93						D				M JMA	
CYA	CSIRO F	110.52	-66.28						F		F4	F4		
DDR	Saitama I	139.18	36.00					H*(11-17)						
DRP	NOAA F	variable	variable						F			F4		
EGB	EC I	-79.78	44.23						H(12-20)		H4(12-16)o	H4(12-16)o		
EIC	NOAA F	-109.45	-27.15	M GV E	M GV E	M GV E	M GV E		F		F4o	F4o	M JMA	
ESP	EC F	-126.55	49.38	M GV E	M GV E	M GV E	M GV E	F	F	M GV E				M GV
ESP	EC I	-126.55	49.38						H(12-20)					
ESP	CSIRO F C13	-126.55	49.38											
ESP	CSIRO F	-126.55	49.38					F	F				M JMA	
EST	EC I	-110.21	51.66									H4(12-16)o		
ETL105	EC I	-104.99	54.35						H(12-20)		H4(12-16)o	H4(12-16)o		
FIK	LSCE F	25.70	35.32						F					
FRD040	EC I	-81.57	49.88	M GV E	M GV E	M GV E	M GV E		H(12-20)		H4(12-16)o	H4(12-16)o		
GMI	NOAA F	144.78	13.43	M GV E	M GV E	M GV E	M GV E	F	F	M GV E	F4o	F4o	M JMA	M GV
GOZ	NOAA F	14.18	36.05						F				M JMA	

Site name[a]	Laboratory[b]	Lon	Lat	TRCom	CCAM	MATCH	RIGC	JENA s96_v3.5	MACC-II	NICAM -TM	CT2011 _oi	CTE2013	JMA	LSCE ana
GSN	SEES I	126.15	33.28	M GV E	M GV E	M GV E	M GV E							
HAT	NIES I	123.80	24.05	M GV E	M GV E	M GV E			H(12-20)					
HBA	NOAA F	-26.50	-75.58	M GV E	M GV E	M GV E	M GV E	F	F	M GV E	F4	F4	M JMA	M GV
HDP	NCAR I	-111.65	40.56									H(0-4)o		
HPB	NOAA F	11.0	47.78						F		F4o	F4o		
HUN	NOAA F	16.65	46.95	M GV E	M GV E	M GV E	M GV E	F	F		F4o			M GV
HUN048	HMS I	16.65	46.95	M GV E										
HUN115	HMS I	16.65	46.95	M GV E				H*(11-17)	H(12-20)			H4(12-16)o		
ICE	NOAA F	-20.15	63.25	M GV E	M GV E	M GV E	M GV E	F	F	M GV E	F4o	F4o	M JMA	M GV
ITN	NOAA F	-77.38	35.35						F					
ITN496	NOAA I	-77.38	35.35											
IZO	AEMET I	-16.48	28.30	M GV E	M GV E	M GV E	M GV E		H(1-6)	M GV E		H(20-8)o	M JMA	
IZO	NOAA F	-16.48	28.30	M GV E				F	F					M GV
JBN	PNRA/DNA I	-58.82	-62.23	M GV E	M GV E	M GV E	M GV E		H(12-20)	M GV E			M JMA	M GV
JFJ	Univ Bern I	7.98	46.55						H(1-6)			H(2-6)o		
JFJ	Univ Bern F	7.98	46.55						F					
KAS	Univ Poland I	19.98	49.22						H(1-6)					
KER	SIO F	-177.15	-29.03					F						
KEY	NOAA F	-80.20	25.67	M GV E	M GV E	M GV E	M GV E	F	F	M GV E	F4o	F4o	M JMA	M GV
KOT	MGO I	137.87	76.00						D					
KPS	HMS I	19.55	46.97						H(12-20)					
KUM	NOAA F	-154.82	19.52	M GV E	M GV E	M GV E	M GV E	F	F	M GV E	F4o	F4o	M JMA	M GV
KUM	SIO F	-154.82	19.52	M GV E				F						
KZD	NOAA F	77.57	44.45		M GV E	M GV E			F		F4o	F4o		M GV
KZM	NOAA F	77.88	43.25		M GV E	M GV E			F	M GV E	F4o	F4o		M GV
LEF	NOAA F	-90.27	45.93					F						
LEF396	NOAA I	-90.27	45.93						H(12-20)	M GV E	H4(12-16)o	H4(12-16)o		

Site name[a]	Laboratory[b]	Lon	Lat	TRCom	CCAM	MATCH	RIGC	JENA s96_v3.5	MACC-II	NICAM -TM	CT2011 _oi	CTE2013	JMA	LSCE ana
LEF_01P0 (396m)	NOAA F	-90.27	45.93								F4o			
LJO	SIO F	-117.30	32.90	M GV E	M GV E	M GV E		F				F4o		
LLB010	EC I	-112.45	54.95								H4(12-16)o	H4(12-16)o		
LLN	NOAA F	120.86	23.46						F					
LMP	NOAA F	12.62	35.52					F	F		F4o	F4o		
LMP	ENEA F	12.62	35.52					F						M GV
LMP	ENEA I	12.62	35.52											
LMU0079	IC3 I	1.83	41.58											
LPO	LSCE F	-3.58	48.80						F			F4o		
LUT0060	RUG-CIO I	6.37	52.38									H4(12-16)o		
MAA	CSIRO F	62.87	-67.62	M GV E	M GV E	M GV E	M GV E	F	F	M GV E	F4	F4	M JMA	M GV
MAA	CSIRO F C13	62.87	-67.62		M	M								
MBC	NOAA F	-119.35	76.25						F				M JMA	
MEX	NOAA F	-97.31	18.98									F4o		
MHD	NOAA F	-9.90	53.33	M GV E	M GV E	M GV E	M GV E	F	F	M GV E	F4o	F4o	M JMA	M GV
MHD	LSCE I	-9.90	53.33						H(12-20)					
MHD	LSCE F	-9.90	53.33						F					
MHDCBC	LSCE I	-9.90	53.33	M GV E										
MHDRBC	LSCE I	-9.90	53.33	M GV E										
MID	NOAA F	-177.37	28.22	M GV E	M GV E	M GV E	M GV E	F	F	M GV E	F4o	F4o	M JMA	M GV
MKN	NOAA F	37.30	-0.05						F		F4o	F4o		
MLO	NOAA I	-155.58	19.53	M GV E	M GV E	M GV E	M GV E	H*	H(1-6)	M GV E	H4(0-4)	H4(0-4)	M JMA	
MLO	NOAA F	-155.58	19.53	M GV E				F	F		F4o			M GV
MLO	SIO F	-155.58	19.53	M GV E				F						
MLO	CSIRO F			M GV E										
MLO	CSIRO F C13	-155.58	19.53		M	M								
MNM	JMA I	153.97	24.30	M GV E	M GV E	M GV E	M GV E	H*(11-17)	H(12-20)	M GV E			M JMA	

Site name[a]	Laboratory[b]	Lon	Lat	TRCom	CCAM	MATCH	RIGC	JENA s96_v3.5	MACC-II	NICAM -TM	CT2011 _oi	CTE2013	JMA	LSCE ana
MQA	CSIRO F	158.97	-54.48	M GV E	M GV E	M GV E	M GV E	F	F	M GV E	F4	F4	M JMA	M GV
MQA	CSIRO F C13	158.97	-54.48		M	M								
NAT	NOAA F	-35.26	-5.51									F4o		
NMB	NOAA F	15.03	-23.58						F		F4o	F4o	M JMA	
NOV030	NIES F	83.00	55.00											
NOV040	NIES F	83.00	55.00											
NOV055	NIES F	83.00	55.00											
NOV070	NIES F	83.00	55.00											
NWR	NOAA F	-105.58	40.05	M GV E	M GV E	M GV E	M GV E	F	F	M GV E	F4o	F4o		M GV
NWR_01P0	NOAA F	-105.58	40.05										M JMA	
NWR	NCAR I	-105.58	40.05								H4(0-4)o	H4(0-4)o		
OBN	NOAA F	36.60	55.10								F4o	F4o		
OXK	NOAA F	11.80	50.03						F		F4o	F4o		
PAL	FMI I	24.12	67.97						H(12-20)			H(12-16)o		M GV
PAL	NOAA F	24.12	67.97						F		F4o		M JMA	
PDM	LSCE F	0.13	42.93						F			F4o		
POC ships	NOAA F	168 to -131	-35 to 45								F4	F4		
POCS35	NOAA F	168.00	-35.00						F				M JMA	
POCS30	NOAA F	169.00	-30.00		M GV E	M GV E			F	M GV E			M JMA	M GV
POCS25	NOAA F	174.00	-25.00		M GV E	M GV E	M GV E		F	M GV E			M JMA	
POCS20	NOAA F	-178.50	-20.00	M GV E	M GV E	M GV E			F	M GV E			M JMA	M GV
POCS15	NOAA F	-178.00	-15.00	M GV E	M GV E	M GV E	M GV E		F	M GV E			M JMA	
POCS10	NOAA F	-174.00	-10.00	M GV E	M GV E	M GV E	M GV E		F	M GV E			M JMA	M GV
POCS05	NOAA F	-168.00	-5.00	M GV E	M GV E	M GV E	M GV E		F	M GV E			M JMA	
POC000	NOAA F	-163.00	0.00	M GV E	M GV E	M GV E	M GV E		F	M GV E			M JMA	M GV
POCN05	NOAA F	-158.00	5.00	M GV E	M GV E	M GV E	M GV E		F	M GV E			M JMA	
POCN10	NOAA F	-152.00	10.00		M GV E	M GV E	M GV E		F	M GV E			M JMA	M GV

Site name[a]	Laboratory[b]	Lon	Lat	TRCom	CCAM	MATCH	RIGC	JENA s96_v3.5	MACC-II	NICAM -TM	CT2011 _oi	CTE2013	JMA	LSCE ana
POCN15	NOAA F	-147.00	15.00	M GV E	M GV E	M GV E	M GV E		F	M GV E			M JMA	
POCN20	NOAA F	-140.00	20.00	M GV E	M GV E	M GV E	M GV E		F	M GV E			M JMA	M GV
POCN25	NOAA F	-134.00	25.00		M GV E	M GV E	M GV E		F	M GV E			M JMA	
POCN30	NOAA F	-126.00	30.00	M GV E	M GV E	M GV E	M GV E		F	M GV E			M JMA	M GV
PRS	CESI/RICERCA I	7.70	45.93						H(1-6)				M JMA	M GV
PSA	NOAA F	-64.00	-64.92	M GV E	M GV E	M GV E	M GV E	F	F	M GV E	F4	F4	M JMA	
PSA	SIO F	-64.00	-64.92	M GV E				F						
PTA	NOAA F	-124.72	38.95						F		F4o	F4o		
PUY	LSCE I	3.00	45.80						H(1-6)					
PUY	LSCE F	3.00	45.80						F					
RPB	NOAA F	-59.43	13.17	M GV E	M GV E	M GV E	M GV E	F	F	M GV E	F4o	F4o	M JMA	M GV
RYO	JMA I	141.83	39.03	M GV E	M GV E	M GV E	M GV E	H*(11-17)	H(12-20)				M JMA	M GV
SAN	IPEN	-54.95	-2.85									F4o		
SBL	EC I	-60.02	43.93						H(12-20)		H4(12-16)o		M JMA	
SCH	UBA/UHEI-IUP I	8.00	48.00		M GV E	M GV E		H*(23-5)	H(12-20)					
SCH	Univ Heid. F	8.00	48.00						F				M JMA	M GV
SCSN03	NOAA F	105.00	3.00						F				M JMA	
SCSN06	NOAA F	107.00	6.00						F				M JMA	
SCSN09	NOAA F	109.00	9.00						F				M JMA	
SCSN12	NOAA F	111.00	12.00						F				M JMA	
SCSN15	NOAA F	113.00	15.00						F				M JMA	
SCSN18	NOAA F	115.00	18.00						F				M JMA	
SCSN21	NOAA F	117.00	21.00						F				M JMA	
SCT	NOAA F	-81.83	33.41											
SCT305	NOAA I	-81.83	33.41								H4(12-16)o	H4(12-16)o		
SEY	NOAA F	55.17	-4.67	M GV E	M GV E	M GV E	M GV E	F	F	M GV E	F4	F4	M JMA	M GV

Site name[a]	Laboratory[b]	Lon	Lat	TRCom	CCAM	MATCH	RIGC	JENA s96_v3.5	MACC-II	NICAM -TM	CT2011 _oi	CTE2013	JMA	LSCE ana
SGP	NOAA F	-97.49	36.73						F		F4o			
SGP060	LBNL I	-97.50	36.78								H4(14-18)o	H4(14-18)o		
SHIP (Ryofu maru, Keifu maru)	JMA I	127.5 to 167.5	-2.5 to 42.5										M JMA 5	
SHM	NOAA F	174.10	52.72	M GV E	M GV E	M GV E	M GV E	F	F	M GV E	F4o	F4o	M JMA	M GV
SIH	Tohoku U F	123.83	24.12						F					
SIS	CSIRO F	-1.17	60.17					F	F		F4o	F4o	M JMA	M GV
SIS	MPI BGC F	-1.17	60.17					F						
SMO	NOAA F	-170.57	-14.25	M GV E	M GV E	M GV E	M GV E	F	F	M GV E	F4o		M JMA	M GV
SMO	NOAA I	-170.57	-14.25	M GV E				H*	H(12-20)		H4(12-16)	H4(12-16)		
SMO	SIO F	-170.57	-14.25	M GV E				F						
SNB	EEA I	12.95	47.05						H(1-6)					
SNP017	NOAA I	-78.35	38.62								H4(0-4)o	H4(0-4)o		
SPL	NCAR I	-106.73	40.45								H4(0-4)o	H4(0-4)o		
SPO	NOAA I	-24.80	-89.98	M GV E	M GV E	M GV E	M GV E	H*	H(1-6)	M GV E	H4(12-16)	H4(12-16)	M JMA	
SPO	CSIRO F	-24.80	-89.98	M GV E										
SPO	CSIRO F C13	-24.80	-89.98		M	M								
SPO	NOAA F	-24.80	-89.98	M GV E				F	F		F4o			M GV
SPO	SIO F	-24.80	-89.98	M GV E				F						
STC	NOAA F	-35.00	-54.00										M JMA	
STM	NOAA F	2.00	66.00	M GV E	M GV E	M GV E			F	M GV E	F4o	F4o	M JMA	M GV
STMEBC	NOAA F	2.00	66.00	M GV E			M GV E							
STR_01P0	NOAA F	-122.45	37.76								F4o	F4o		
SUM	NOAA F	-38.48	72.58						F		F4o	F4o	M JMA	
SUR	NIES F	73.00	61.00					F						
SUR030	NIES F	73.00	61.00											
SUR040	NIES F	73.00	61.00											

Site name[a]	Laboratory[b]	Lon	Lat	TRCom	CCAM	MATCH	RIGC	JENA s96_v3.5	MACC-II	NICAM -TM	CT2011 _oi	CTE2013	JMA	LSCE ana
SUR055	NIES F	73.00	61.00											
SUR070	NIES F	73.00	61.00											
SYK1500	MPI-BGC	52.17	61.23											M GV
SYK1500	MPI-BGC	52.17	61.23											M GV
SYO	NIPR I	39.58	-69.00				M GV E			M GV E		D	M JMA	
SYO	NOAA F	39.58	-69.00	M GV E	M GV E	M GV E			F		F4			M GV
TAP	NOAA F	126.13	36.73	M GV E	M GV E	M GV E	M GV E		F		F4o	F4o		M GV
TDF	NOAA F	-68.48	-54.87	M GV E	M GV E	M GV E	M GV E	F	F	M GV E	F4	F4o	M JMA	
TER	MGO F	35.2	69.2										M JMA	
THD	NOAA F	-124.15	41.05						F		F4o	F4o		
TKB	MRI I	140.13	36.05						H(12-20)					
TRM	LSCE F	54.52	-15.88						F					
ULB	NOAA F	106	47.4									F4o		
UTA	NOAA F	-113.72	39.90	M GV E	M GV E	M GV E	M GV E	F	F	M GV E	F4o	F4o		M GV
UUM	NOAA F	111.10	44.45	M GV E	M GV E	M GV E	M GV E	F	F		F4o	F4o	M JMA	M GV
WBI379	NOAA I	-91.35	41.72								H4(12-16)o	H4(12-16)o		
WBI_01P0 (379m)	NOAA F	-91.35	41.72								F4o			
WES	UBA/UHEI-IUP I	8.00	55.00						H(12-20)					
WGC483	NOAA I	-121.49	38.26								H4(12-16)o	H4(12-16)o		
WGC_01P0 (483m)	NOAA F	-121.49	38.26								F4o			
WIS	NOAA F	34.88	31.13	M GV E	M GV E	M GV E	M GV E	F	F	M GV E	F4o	F4o	M JMA	M GV
WKT009	NOAA I	-97.62	31.32											
WKT457	NOAA I	-97.62	31.32						H(12-20)		H4(12-16)o	H4(12-16)o		
WKT_01P0 (457m)	NOAA F	-97.62	31.32								F4o			
WLG	NOAA F	100.90	36.29	M GV E	M GV E	M GV E	M GV E		F	M GV E	F4o	F4o	M JMA	M GV

Site name[a]	Laboratory[b]	Lon	Lat	TRCom	CCAM	MATCH	RIGC	JENA s96_v3.5	MACC-II	NICAM -TM	CT2011 _oi	CTE2013	JMA	LSCE ana
WLG	CAMS I	100.90	36.29	M GV E										
WPC	NOAA F	167.9	-30.67											
WPON30	NIES F	146.00	30.00	M GV E			M GV E			M GV E			M JMA	M GV
WPON25	NIES F	146.00	25.00	M GV E			M GV E			M GV E			M JMA	
WPON20	NIES F	146.00	20.00	M GV E			M GV E			M GV E			M JMA	M GV
WPON15	NIES F	146.00	15.00	M GV E			M GV E			M GV E			M JMA	
WPON10	NIES F	146.00	10.00	M GV E			M GV E			M GV E			M JMA	
WPON05	NIES F	146.00	5.00	M GV E			M GV E			M GV E			M JMA	
WPO000	NIES F	146.00	0.00	M GV E			M GV E			M GV E			M JMA	M GV
WPOS05	NIES F	146.00	-5.00	M GV E			M GV E			M GV E			M JMA	
WPOS10	NIES F	146.00	-10.00	M GV E						M GV E			M JMA	
WPOS15	NIES F	146.00	-15.00	M GV E						M GV E			M JMA	
WPOS20	NIES F	146.00	-20.00	M GV E						M GV E			M JMA	M GV
WPOS25	NIES F	146.00	-25.00							M GV E			M JMA	
WSA	EC I	-60.02	49.93								H4(12-16)o	H4(12-16)o		
YAK030	NIES F	130.00	62.00											
YON	JMA I	123.02	24.47				M GV E		H(12-20)	M GV E			M JMA	
ZEP	NOAA F	11.88	78.90		M GV E	M GV E	M GV E	F	F	M GV E	F4o	F4o		M GV
ZEP	Stockholm Univ I	11.88	78.90						H(12-20)				M JMA	
ZOT035	MPI-BGC	89.38	60.75											M GV
ZOT015	MPI-BGC	89.38	60.75											M GV

Old inversion results used by other RECCAP synthesis: system differences and figures

This appendix provides additional figures showing the results that were obtained with the inversion submissions initially provided to the other RECCAP papers. The flux estimates were different for 5 inversions:

- **JENA**: Compared to the present version s96_v3.5 shown in this paper, some other RECCAP publications used version s96_v3.3 that also allowed adjustments to the time-mean ocean fluxes [and had extra degrees of freedom for large-scale ocean seasonality]. It also used an older ocean inversion as prior (Gloor et al., 2003). Version s96_v3.3 thus had substantially different long-term mean ocean fluxes: around 0.5 PgC/yr versus -1.8 PgC/yr in the current version s96_v3.5 for the period 2001-2004. However, the interannual variability is nearly identical to the present version over the common period [small changes originate from minor alterations in the list of sites due to data availability: the sites WPO, JBN, BME, and STM have been removed, while DDR has been added].
- **MACC-II:** An earlier version of this product was referenced as "LSCEv" in other RECCAP publications (corresponding to Chevallier et al., 2010). The differences with MACC-II v11.2 mainly result from (i) an update of the prior natural fluxes with a more recent land surface model version (http://forge.ipsl.jussieu.fr/orchidee/wiki/Documentation/ORCHIDEE_DOC, accessed 17 July 2013), (ii) an update of the prior error statistics to fit this new version, based on an extended flux measurement database (Chevallier et al. 2012), (iii) the suppression of the interannual variability of the prior natural fluxes, (iv) the extension of the inversion backward to 1979 and forward to 2011 with a novel parallelization approach (Chevallier 2013). The new estimated fluxes have a larger ocean uptake (mainly in the south) and a smaller tropical land uptake and show few small changes in the IAV. The long-term trends also slightly changed with and increased tropical land carbon uptake in the 2000s in MACC-II.
- **CT2011_oi**: The CT2011_oi updates the time period of the original inversion (CT2009), to 2001-2010. It corresponds to a revision of CT2011 in response to a

bug discovered in the atmospheric transport model (TM5). CT2011_oi is derived from a suite of four different inversions, each using a different set of prior fluxes (see http://www.esrl.noaa.gov/gmd/ccgg/carbontracker/documentation_assim.html#ct_doc for more information). The new product "CT2011_oi" thus replaces the previous product "CT2009" with similar long-term mean fluxes (only a slight increase of the northern land uptake) and with slightly larger amplitude of the flux IAV.

- **CTE2013**: The CTE2013 updates the time period of the original inversion (CTE2008) to 2001-2010 rather than ending in 2007. Also, the specific focus on Europe from CTE2008 has been removed: CTE2013 has no extra ecoregions and no extra European time series) in favor of a more globally oriented setup. This means that an ObsPack was used in the assimilation with a set of sites more typical for the CarbonTracker systems. Finally, the transport model TM5 had a higher resolution in the CTE2013 release with global 3x2, and zoom regions of 1x1 over Europe and North America. The CTE2013 provides similar long-term mean fluxes and a slightly larger amplitude of the flux IAV.
- **NICAM**: The site list of the new version used in this paper is different from that of the older version. Although the older version used 103 site measurements, the number of sites has reduced to 71 in the present version. The principal difference is that Siberian aircraft data were not used in the present version. Other sites were also taken off to reduce redundancy (some sites were located nearby to each other in the older version). The new version lead to smaller land uptake in North America compensated by a larger land uptake in the tropics. Similar interannual flux variations (IAV) are found with slightly smaller amplitude in the Tropics and the North, especially in North America and North Asia. The new results are more coherent with the other inversions for North America.

We present below a few similar figures to those in the core paper but with the old flux estimates for these 5 inversions.

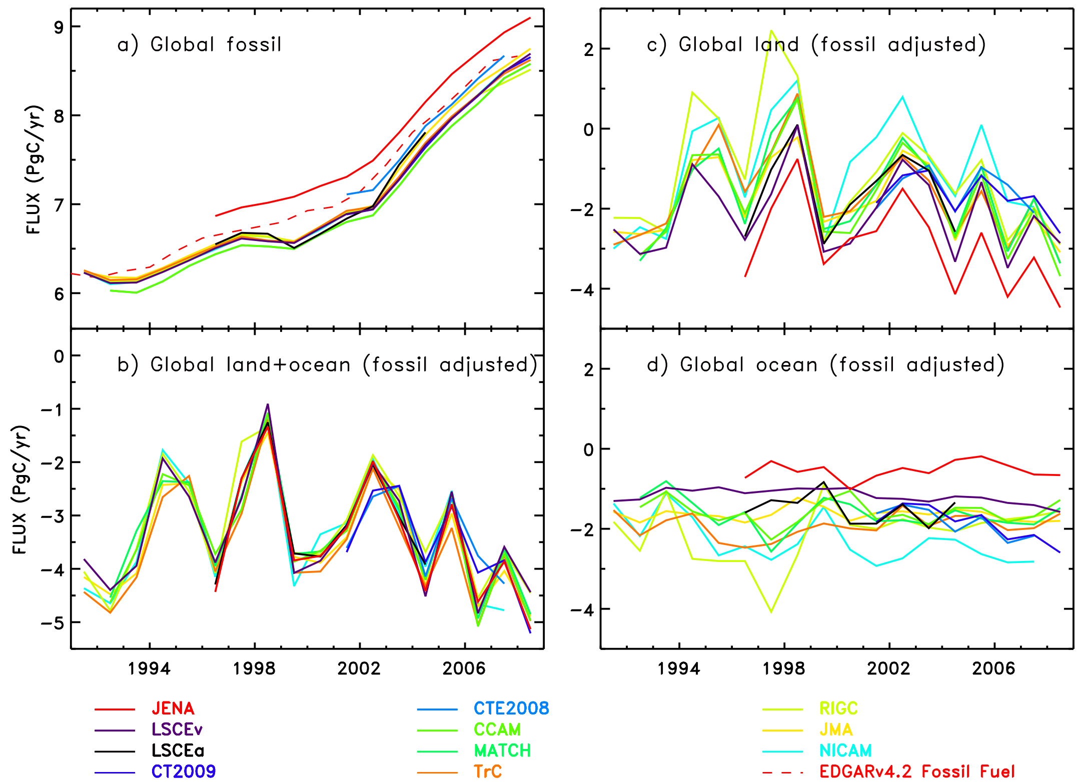

Figure S9 (Same as figure 2 but with the old submissions): Annual mean posterior flux of the individual participating inversions for a) fossil fuel emission, b) natural “fossil corrected” global total carbon exchange, c) natural “fossil corrected” total land and d) natural “fossil corrected” total ocean fluxes.

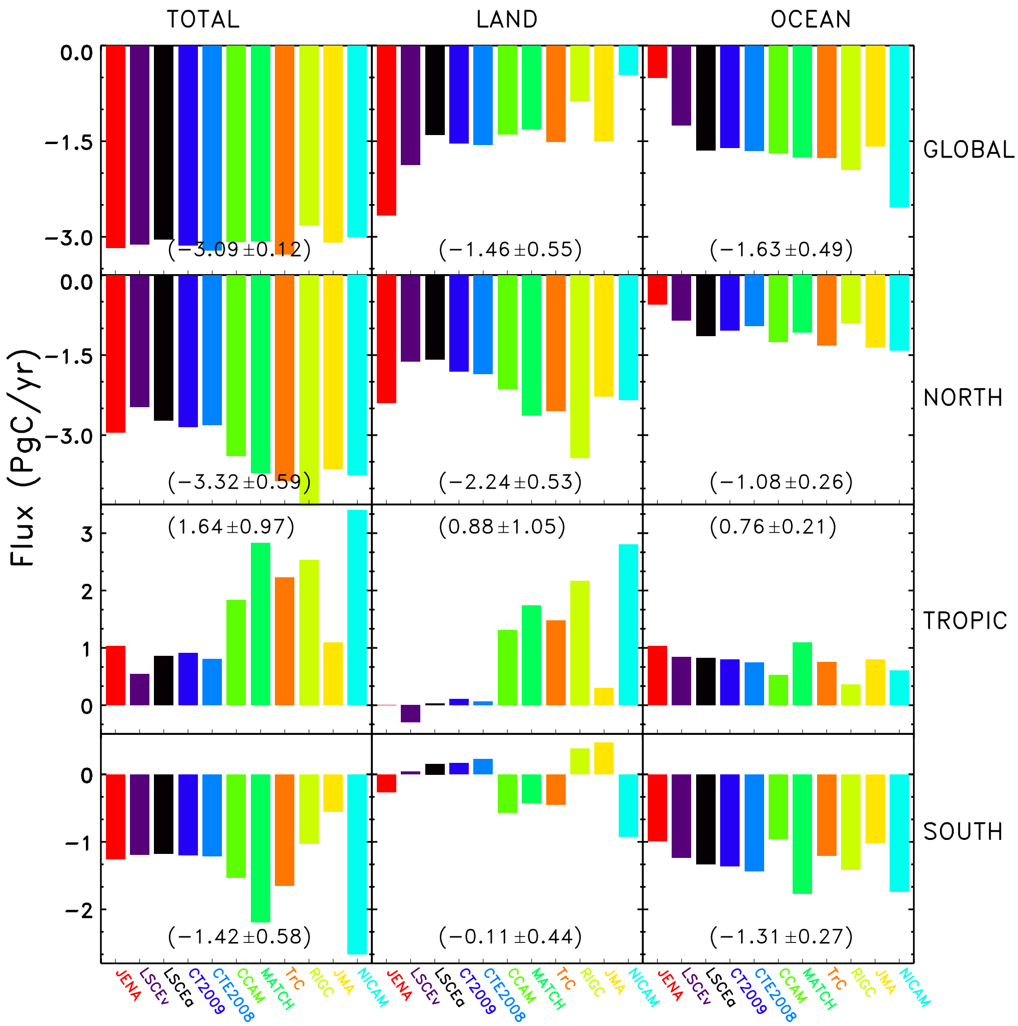

Figure S10 (Same as figure 4 but with the old submissions): Mean natural fluxes for the period 2001-2004. Shown here are total (first column), natural "fossil corrected" land (second column) and natural ocean (third column) carbon exchange aggregated over the Globe (top row), the North (2nd row), the Tropics (3rd row) and the South (bottom row), with the three regions divided by approximately 25°N and 25°S (but modified over land areas to keep regional estimates (e.g. northern Africa) in one region; see figure S7). Numbers in parentheses represent the mean flux and the standard deviation across all inversions.

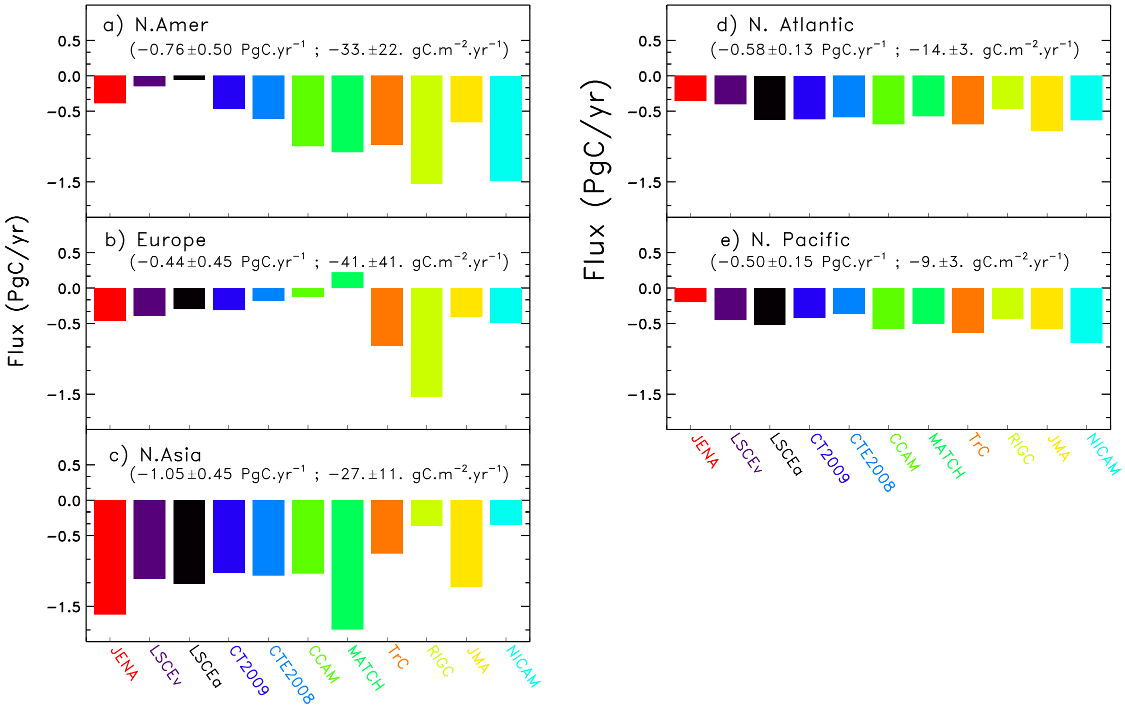

Figure S11 (Same as figure 5 but with the old submissions): Breakdown of the Northern hemisphere fluxes into a) North America, b) Europe, c) North Asia, d) N. Atlantic, and e) N. pacific. Numbers in parenthesis represent the mean flux and the standard deviation across all inversions.

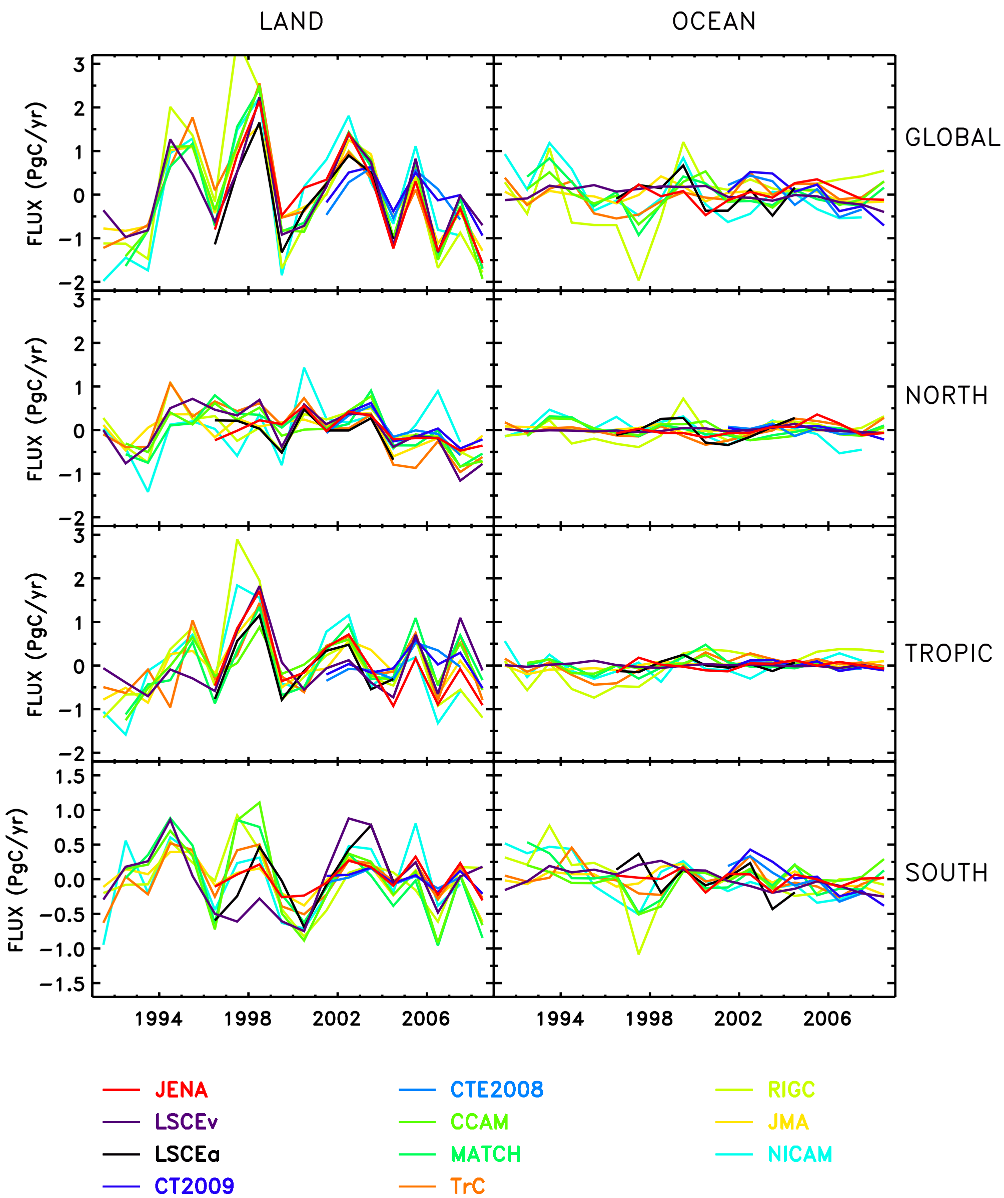

Figure S12 (Same as figure 6 but with the old submissions): Annual mean anomalies of the individual participating inversion posterior flux estimates. Shown here are the fossil corrected natural land (first column) and natural ocean (second column) carbon exchange for the same regions as Figure 4: the Globe, north (> 25N), tropics (25S-25N) and south (< 25S).

References

Andres, R. J., Marland, G., Fung, I., and Matthews, E.: A 1° x 1° distribution of carbon dioxide emissions from fossil fuel consumption and cement manufacture, 1950–1990, Global Biogeochem. Cycles, 10, 419–429, 1996.

Andres, R.J., Boden, T. A., and Marland., G.: Monthly Fossil-Fuel CO_2 Emissions: Mass of Emissions Gridded by One Degree Latitude by One Degree Longitude. Carbon Dioxide Information Analysis Center, Oak Ridge National Laboratory, U.S. Department of Energy, Oak Ridge, Tenn., U.S.A. doi: 10.3334/CDIAC/ffe.MonthlyMass.2009, 2009.

Baker, D. F., Law, R. M., Gurney, K. R., Rayner, P., Peylin, P., Denning, A.S., Bousquet, P., Bruhwiler, L., Chen, Y.-H., Ciais, P., Fung, I. Y., Heimann, M., John, J., Maki, T., Maksyutov, S., Masarie, K., Prather, M., Pak, B., Taguchi, S., and Zhu, Z.: TransCom 3 inversion intercomparison: Impact of transport model errors on the interannual variability of regional CO_2 fluxes, 1988–2003, Global Biogeochem. Cycles, 20, GB1002, doi:10.1029/2004GB002439, 2006.

Brenkert, A. L.: Carbon dioxide emission estimates from fossil-fuel burning, hydraulic cement production, and gas flaring for 1995 on a one degree grid cell basis, Rep. NDP-058A, Carbon Dioxide Infor. Anal. Cent., Oak Ridge Natl. Lab., Oak Ridge, Tenn, 1998.

Chevallier, F., Fisher, M., Peylin, P., Serrar, S., Bousquet, P., Bréon, F.-M., Chédin, A., and Ciais, P.: Inferring CO_2 sources and sinks from satellite observations: Method and application to TOVS data, J. Geophys. Res., 110, D24309, doi:10.1029/2005JD006390, 2005.

Chevallier, F., Ciais, P., Conway, T.J., Aalto, T., Anderson, B. E., Bousquet, P., Brunke, E. G., Ciattaglia, L., Esaki, Y., Fröhlich, M., Gomez, A. J., Gomez-Pelaez, A. J., Haszpra, L., Krummel, P., Langenfelds, R., Leuenberger, M., Machida, T., Maignan, F., Matsueda, H., Morguí, J. A., Mukai, H., Nakazawa, T., Peylin, P., Ramonet, M., Rivier, L., Sawa, Y., Schmidt, M., Steele, P., Vay, S. A., Vermeulen, A. T., Wofsy, S., and Worthy, D.: CO_2 surface fluxes at grid point scale estimated from a global 21 year reanalysis of atmospheric measurements, J. Geophys. Res., 115, D21307, doi:10.1029/2010JD013887, 2010.

Chevallier, F., T. Wang, P. Ciais, F. Maignan, M. Bocquet, A. Arain, A. Cescatti, J.-Q. Chen, H. Dolman, B. E. Law, H. A. Margolis, L. Montagni, and E. J. Moors: What eddy-covariance flux measurements tell us about prior errors in CO_2-flux inversion schemes. Global Biogeochem. Cy., 26, GB1021, doi:10.1029/2010GB003974, 2012.

Chevallier, F.: On the parallelization of atmospheric inversions of CO_2 surface fluxes within a variational framework. Geosci. Model. Dev., 6, 783-790, doi:10.5194/gmd-6-783-2013, 2013.

Enting, I. G.: Inverse Problems in Atmospheric Constituent Transport, Cambridge University Press, 2002.

Francey, R. J., Steele, L. P., Langenfelds, R. L., Lucarelli, M. P., Allison, C. E., Beardsmore, D. J., Coram, S. A., Derek, N., de Silva, F. R., Etheridge, D. M., Fraser, P. J., Henry, R. J., Turner, B., Welch, W. D., Spencer, D. A., and Cooper, L. N.: Global Atmospheric Sampling Laboratory (GASLAB): Supporting and extending the Cape Grim trace gas program, in Baseline Atmospheric Program (Australia) 1993, edited by R. J. Francey, A. L. Dick, and N. A. Derek, pp. 8 – 29, Bur. of Meteorol. and CSIRO, Aspendale, Victoria, Australia, 1996.

Gurney, K. R., Baker, D., Rayner, P., and Denning, S., Interannual variations in continental-scale net carbon exchange and sensitivity to observing networks estimated from atmospheric CO_2 inversions for the period 1980 to 2005, Global Biogeochem. Cycles, 22, GB3025, doi:10.1029/2007GB003082, 2008.

Jacobson, A. R., Gruber, N., Sarmiento, J. L., Gloor, M., and Mikaloff Fletcher, S. E.: A joint atmosphere-ocean inversion for surface fluxes of carbon dioxide: I. Methods and global-scale fluxes, *Global Biogeochemical Cycles*, 21, doi:10.1029/2005GB002556, 2007.

Krinner, G., Viovy, N., de Noblet-Ducoudré, N., Ogée, J., Polcher, J., Friedlingstein, P., Ciais, P., Sitch, S., and Prentice, I. C. : A dynamic global vegetation model for studies of the coupled atmosphere-biosphere system, Global Biogeochem. Cycles, 19, GB1015, doi:10.1029/ 2003GB002199, 2005.

Krol, M.C., Houweling, S., Bregman, B., van den Broek, M., Segers, A., van Velthoven, P., Peters, W., Dentener, F., and Bergamaschi, P.: The two-way nested global chemistry-transport zoom model TM5: algorithm and applications, *Atm. Chem. Phys.*, 5417-432, 2005.

Maksyutov, S., P. K. Patra, R. Onishi, T. Saeki and T. Nakazawa, NIES/FRCGC global atmospheric tracer transport model: description, validation, and surface sources and sinks inversion, J. Earth. Simulator, 9, 3-18, 2008.

Niwa, Y., Machida, T., Sawa, Y., Matsueda, H., Schuck, T. J., Brenninkmeijer, C. A. M., Imasu, R., and Satoh, M., Imposing strong constraints on tropical terrestrial CO_2 fluxes using passenger aircraft based measurements, *J. Geophys. Res.*, 117, D11303, doi:10.1029/2012JD017474, 2012.

Oda, T. and S., Maksyutov, A very high-resolution (1 km ×1 km) global fossil fuel CO2 emission inventory derived using a point source database and satellite observations of nighttime lights, Atmos. Chem. Phys., 11, 543–556, doi:10.5194/acp-11-543-2011, 2011

Olivier, J. G. J., and Berdowski, J. J. M.: Global emissions sources and sinks, in The Climate System, edited by J. Berdowski, R. Guicherit, and B. J. Heij, pp. 33–78, A. A. Balkema, Lisse, Netherlands, 2001.

Patra, P. K., Maksyutov, S., Ishizawa, M., Nakazawa, T., Takahashi, T. and Ukita, J.: Interannual and decadal changes in the sea-air CO_2 flux from atmospheric CO_2 inverse modelling, Global Biogeochem. Cycles, 19, GB4013, 2005.

Peters, W., Jacobson, A. R., Sweeney, C., Andrews, A. E., Conway, T. J., Masarie, K., Miller, J. B., Bruhwiler, L., M. P., Pétron, G., Hirsch, A. I., Worthy, D. E. J., van der Werf, G. R., Randerson, J. T., Wennberg, P. O., Krol, M. C., and Tans, P.P.: An atmospheric perspective on North American carbon dioxide exchange: CarbonTracker, PNAS, 104, 18925-18930, doi:10.1073/pnas.0708986104, 2007.

Peylin P., P. Rayner, P. Bousquet, C. Carouge, F. Hourdin, P. Heinrich, P. Ciais, and AEROCARB contributors, Daily CO_2 flux over Europe from continuous atmospheric measurements: 1, inverse methodology, Atmos. Chem. and Phys., 5, 3173-3186, ISI:000233610300001, 2005.

Piao, S. L., Fang, J. Y., Ciais, P. Peylin, P., Huang, Y., Sitch, S., and Wang, T.: The carbon balance of terrestrial ecosystems in China, Nature, 458, 1009-1014, 2009.

Randerson, J. T., Thompson, M. V., Conway, T. J., Fung, I. Y., and Field, C. B.: The contribution of terrestrial sources and sinks to trends in the seasonal cycle of atmospheric carbon dioxide, Global Biogeochem. Cycles, 11, 535– 560, 1997.

Randerson, J. T., van der Werf, G. R., Giglio, L., Collatz, G. J., and Kasibhatla, P. S.: Global Fire Emissions Database, version 2.1, Oak Ridge Natl. Lab., Oak Ridge, Tenn., doi:10.3334/ORNLDAAC/849, 2007.

Rayner, P. J., Law, R. M., Allison, C. E., Francey, R. J., Trudinger, C. M., and Pickett-Heaps, C.: Interannual variability of the global carbon cycle (1992–2005) inferred by inversion of atmospheric CO_2 and $d^{13}CO_2$ measurements, Global Biogeochem. Cycles, 22, GB3008, doi:10.1029/2007GB003068, 2008.

Takahashi, T., Wanninkhof, R. H., Feely, R. A., Weiss, R. F., Chipman, D. W., Bates, N., Olafsson, J., Sabine, C., and Sutherland, S. C.: Net sea-air CO_2 flux over the global oceans: An improved estimate based on the sea air pCO_2 difference, in Extended Abstracts of the 2nd International CO_2 in the Oceans Symposium, Tsukuba, Japan, January 18– 22, 1999, edited by Y. Nojiri, pp. 9 – 15, Natl. Inst. for Environ. Stud., Tsukuba, Japan, 1999.

Takahashi, T., Sutherland, S. C., Sweeney, C., Poisson, A., Metzl, N., Tillbrook, B., Bates, N., Wanninkhof, R., Feely, R. A., Sabine, C., Olafsson, J., and Nojiri, Y.: Global sea-air CO_2 flux based on climatological surface ocean pCO_2, and seasonal biological and temperature effects, Deep-Sea Res. II, 49, 1601-1622, 2002.

Takahashi, T., Sutherland, S. C., Wanninkhof, R., Sweeney, C., Feely, R. A., Chipman, D. W., Hales, B., Friederich, G., Chavez, F., Sabine, C., Watson, A., Bakker, D. C. E., Schuster, U., Metzl, N., Yoshikawa-Inoue, H., Ishii, M. Midorikawa, T., Nojiri, Y., Kortzinger, A., Steinhoff, T., Hoppema, M., Olafsson, J., Arnarson, T. S., Tillbrook, B., Johannessen, T., Olsen, A., Bellerby, R., Wong, C. S., Delille, B., Bates, N. R., and de Baar, H. J. W.: Climatological mean and decadal change in surface ocean pCO_2 and net sea-air CO_2 flux over the global oceans. Deep-Sea Res. II, 56, 554-577, doi:10.1016/j.dsr2.2008.12.009, 2009.

Van der Werf, G. R., Randerson, J. T., Giglio, L., Collatz, G. J., and Kasibhatla, P. S.: Interannual variability in global biomass burning emission from 1997 to 2004, Atmospheric Chemistry and Physics, 6, 3423-3441. SRef-ID: 1680-7324/acp/2006-6-3423, 2006.